Bifunctional Compounds for Controlling Metal-Mediated Aggregation of the $A\beta_{42}$ Peptide

Anuj K. Sharma,[a] Stephanie T. Pavlova,[a] Jaekwang Kim,[b] Darren Finkelstein,[a] Nicholas J. Hawco,[a] Nigam P. Rath,[c] Jungsu Kim,[b] Liviu M. Mirica[a]*

[a]*Department of Chemistry, Washington University, One Brookings Drive, St. Louis, Missouri 63130-4899*

[b]*Department of Neurology, Washington University School of Medicine, St. Louis, Missouri 63108 and*

[c]*Department of Chemistry and Biochemistry, University of Missouri St. Louis, One University Boulevard, St. Louis, Missouri 63121-4400*

Table of Contents

I. **Table S1.** Crystal data and structure refinement parameters for complexes **1-4**.

compound	**1**	**2**	**3**	**4**
formula	$C_{108}H_{95}B_2Cu_2N_{11}O_4S_2$	$C_{111}H_{133}Cl_4N_{16}O_{40}S_4Zn_4$	$C_{44}H_{40}CuN_6O_4S_2$	$C_{143}H_{139}Cl_2N_{23}O_{23}S_6Zn_6$
formula weight	1823.77	2862.85	844.48	3203.25
crystal system	Triclinic	Monoclinic	Monoclinic	Cubic
space group	*P*-1	$P2_1/n$	$P2_1/c$	*P*a-3
a/Å	13.3302(8)	24.378(2)	17.176(7)	24.3490(9)
b/Å	14.5868(10)	20.8777(16)	11.301(4)	24.3490(9)
c/Å	23.7796(17)	26.115(2)	10.045(4)	24.3490(9)
α/deg	92.590(3)	90.00	90.00	90.00
β/deg	93.906(3)	102.489(3)	96.726(11)°	90.00
γ/deg	103.155(3)	90.00	90.00	90.00
V/Å^3	4483.3(5)	12976.9(19)	1936.6(13)	14435.9(9)
Z	2	4	2	4
D_c/g cm^{-3}	1.351	1.465	1.448	1.474
μ/mm^{-1}	0.584	0.963	0.725	1.181
F_{000}	1984	5932	878	6608
Temp. (K)	100 (2)	100 (2)	100 (2)	100 (2)
data/ restraints/ parameter	18400/1221	24282/1658	3405/261	4277/311
R_1 ($I > 2\sigma(I)$[a]	0.0391	0.0664	0.0662	0.0923
wR_2 (all data)[b]	0.0841	0.1998	0.1918	0.3020
GOF	1.011	1.125	1.048	1.014
Largest diff. peak and hole (e·Å^{-3})	0.433, -0.454	1.525, -1.389	1.956, -2.297	0.568, -1.075

[a] $R = \Sigma||F_0| - |F_c||/\Sigma|F_0|$ [b] $R_w = [\Sigma w(|F_o|-|F_c|^2/\Sigma w(F_o)^2]^{1/2}$

II. Table S2. Drug-like properties of L1 and L2.

Properties	L1	L2	Lipinski's Rule[a]
M.W.	468.5	391.5	≤ 450
clogP	4.046	3.818	≤ 5
HBD	1	1	≤ 5
HBA	6	5	≤ 10
PSA	71.38	58.48	≤ 90 Å^2
logBB	-0.311	-0.155	> -1

[a] MW: molecular weight; clogP: calculated logarithm of the octanol-water partition coefficient; HBD: hydrogen-bond donor atoms; HBA: hydrogen-bond acceptor atoms; PSA: polar surface area; logBB = –0.0148 x PSA + 0.152 x clogP + 0.130 (refs: (a) Lipinski, C. A.; Lombardo, F.; Dominy, B. W.; Feeney, P. J. *Adv. Drug Delivery Rev.* **1997**, *23*, 3-25; (b) Clark, D. E.; Pickett, S. D. *Drug Disc. Today* **2000**, *5*, 49-58).

III. (a) Spectrophotometric titration for L1 and Cu

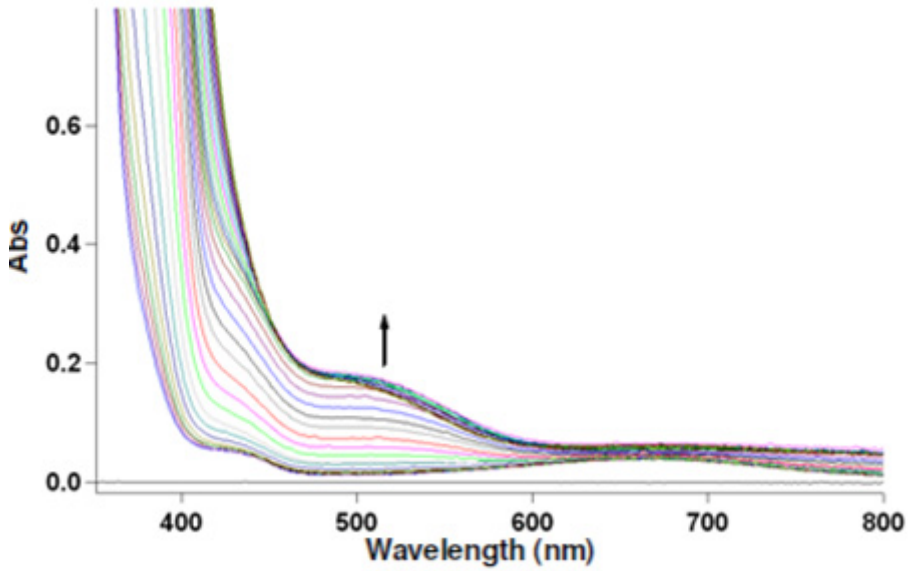

Figure S1. Variable pH-spectrophotometric titration for the L1-Cu^{2+} system (MeOH-H_2O (1:1), [L1] = [Cu] = 0.50 mM, I = 0.1 M NaCl).

(b) Spectrophotometric titration for L2 and Cu^{2+}

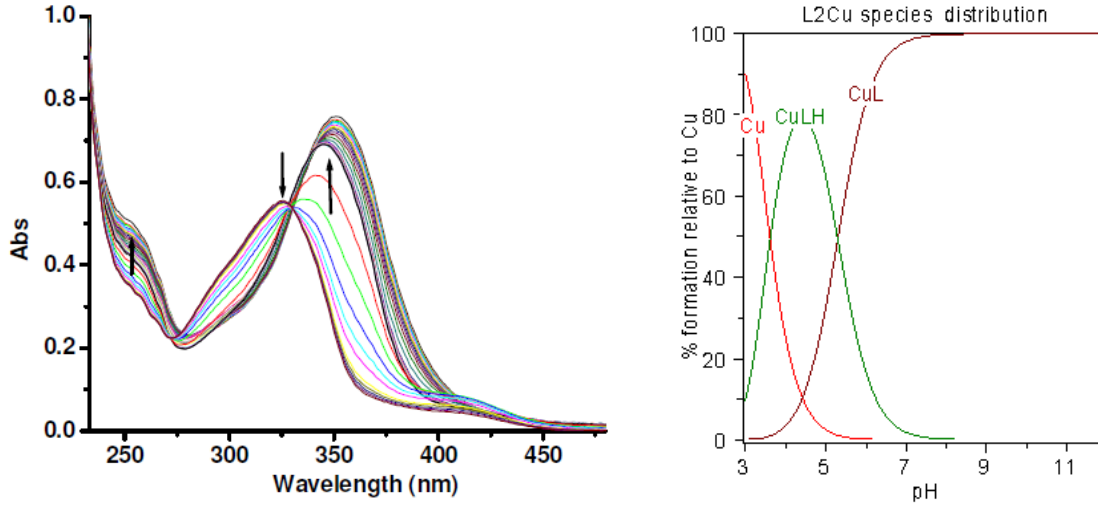

Figure S2. Variable pH (pH 3-11) UV spectra of L2 and Cu^{2+} system ([L2] = [Cu^{2+}] = 50 μM, 25 °C, I = 0.1 M NaCl) and species distribution plot.

(c) Spectrophotometric titration for L2 and Zn^{2+}

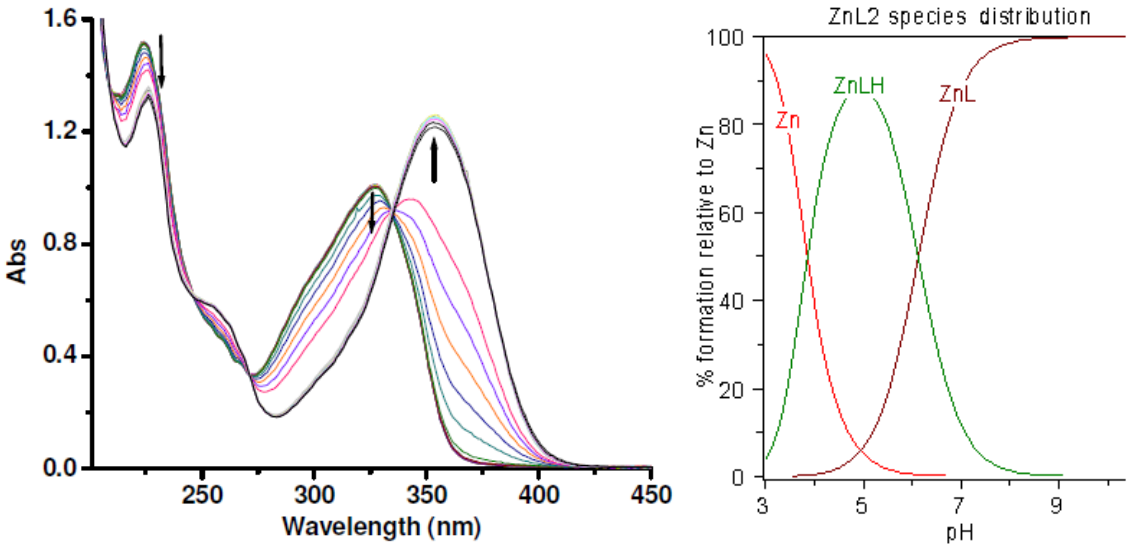

Figure S3. Variable pH (pH 3-11) UV spectra of L2 and Zn^{2+} system ([L2] = [Zn^{2+}] = 50 μM, 25 °C, I = 0.1 M NaCl) and species distribution plot.

IV. Job's plots for solution stoichiometry determination

L1 with Cu:

(a)

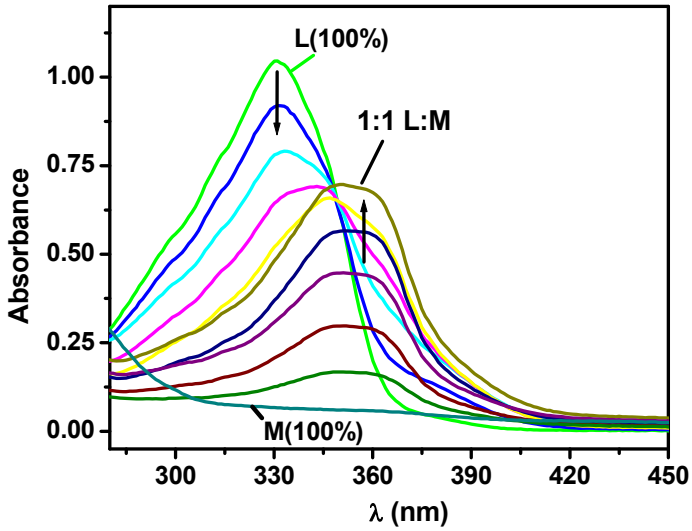

(b)

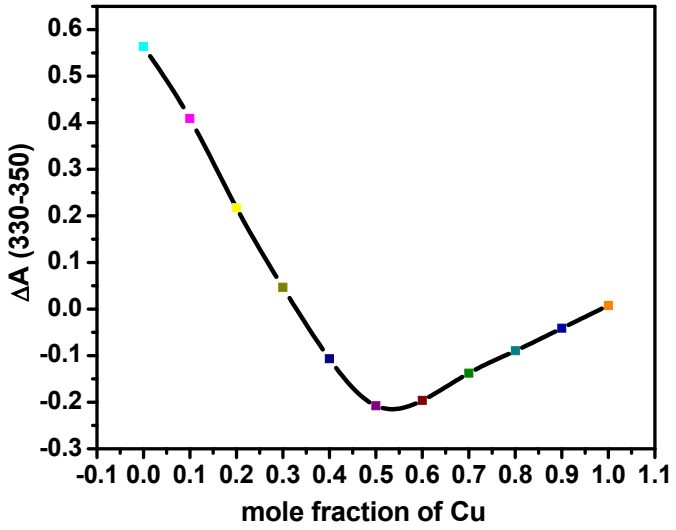

Figure S4. (a) Spectra and (b) Job's plot for L1 and Cu^{2+} in MeCN.

L1 with Zn:

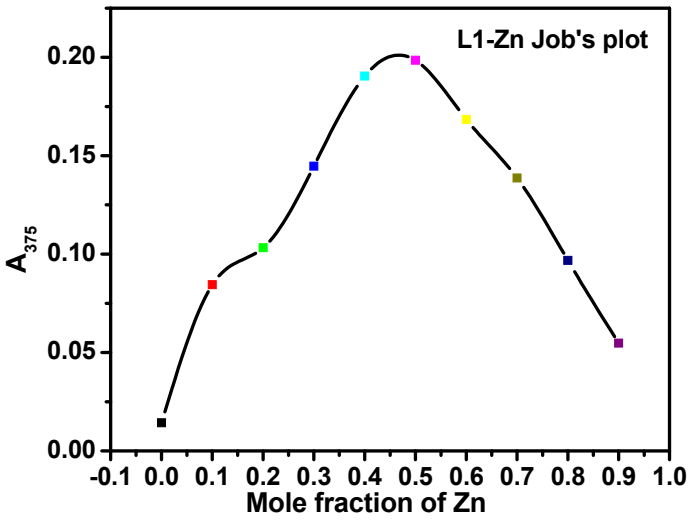

Figure S5. Job's plot for L1 and Zn^{2+} in MeCN.

L2 with Cu:

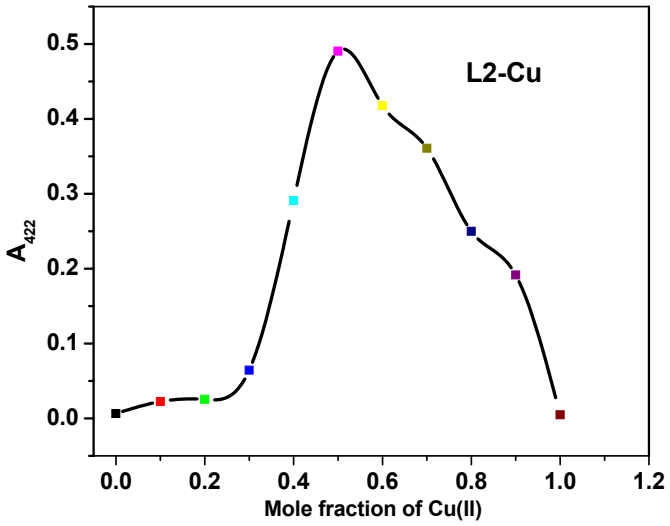

Figure S6. Job's plot for L2 and Cu^{2+} in MeCN.

L2 with Zn:

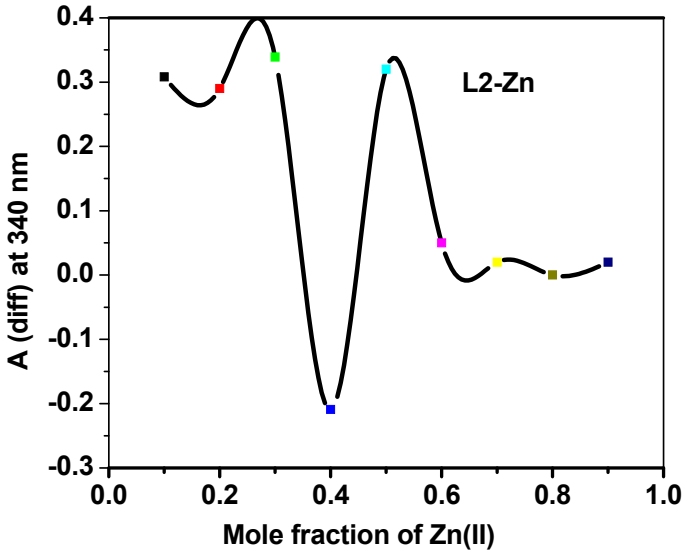

Figure S7. Job's plot for L2 and Zn^{2+} in MeCN.

V. Absorption spectra of L1, L2, and their Cu^{2+} and Zn^{2+} complexes

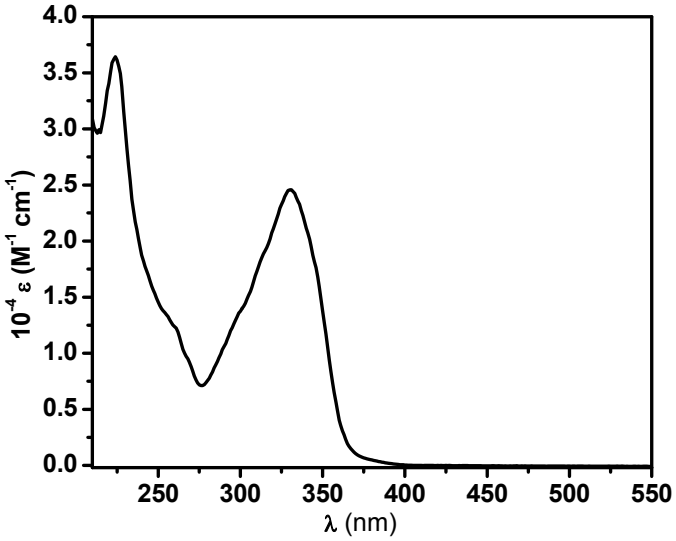

Figure S8. Absorption spectrum of L1 in MeCN.

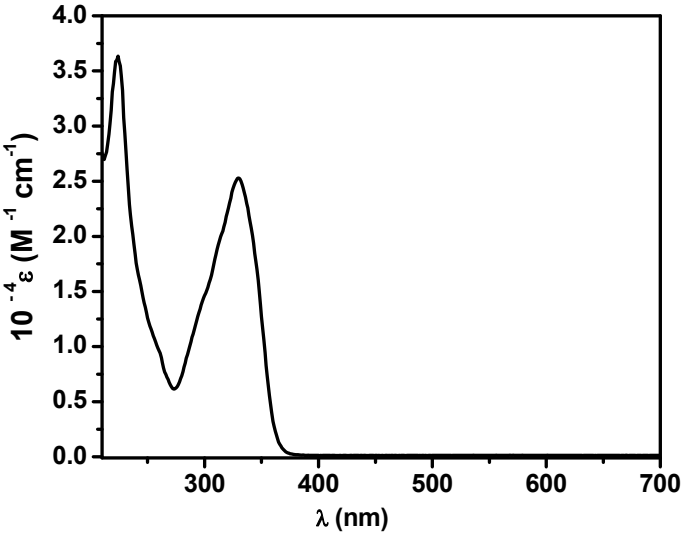

Figure S9. Absorption spectrum of L2 in MeCN.

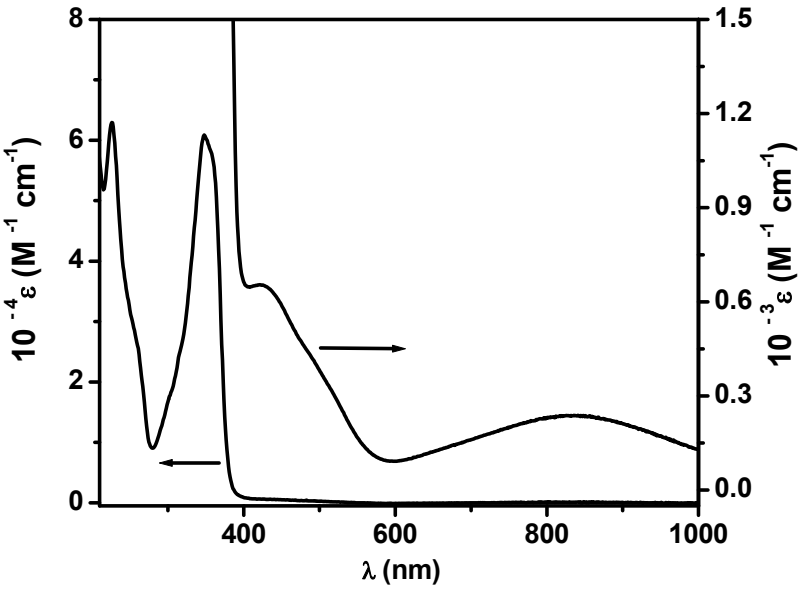

Figure S10. Absorption spectrum of **1** in MeCN.

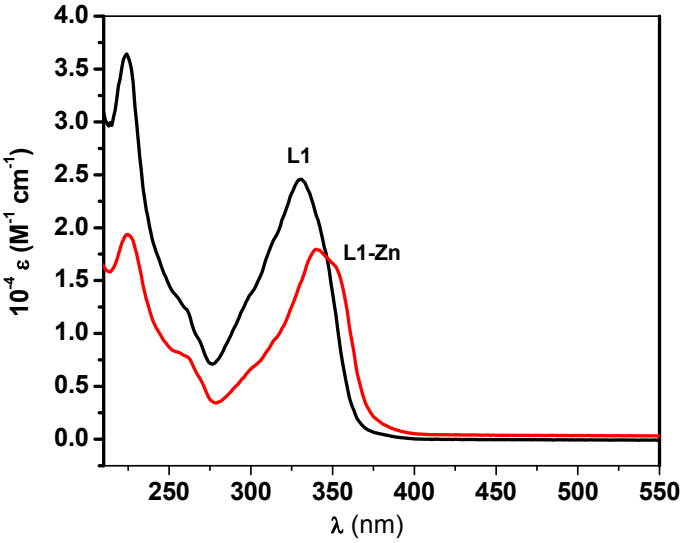

Figure S11. Absorption spectra of L1 and **2** in MeCN.

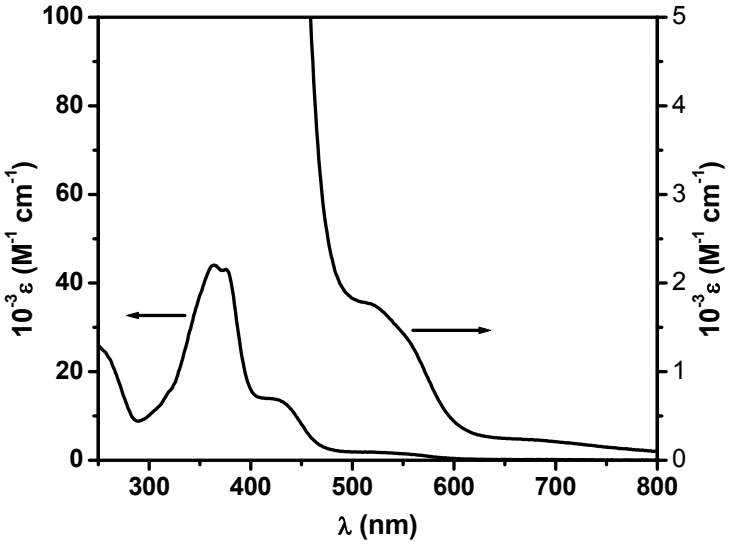

Figure S12. Absorption spectrum of **3** in CH_2Cl_2.

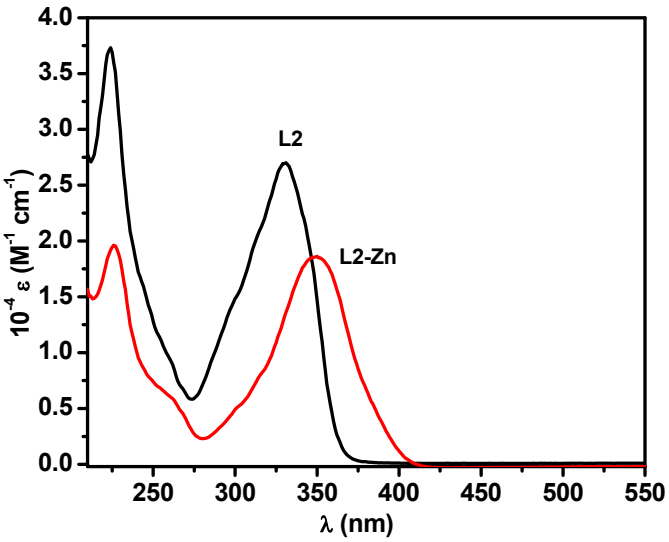

Figure S13. Absorption spectra of L2 and **4** in MeCN.

VI. Fluorescence spectra of L1, L2, and their Cu^{2+} and Zn^{2+} complexes

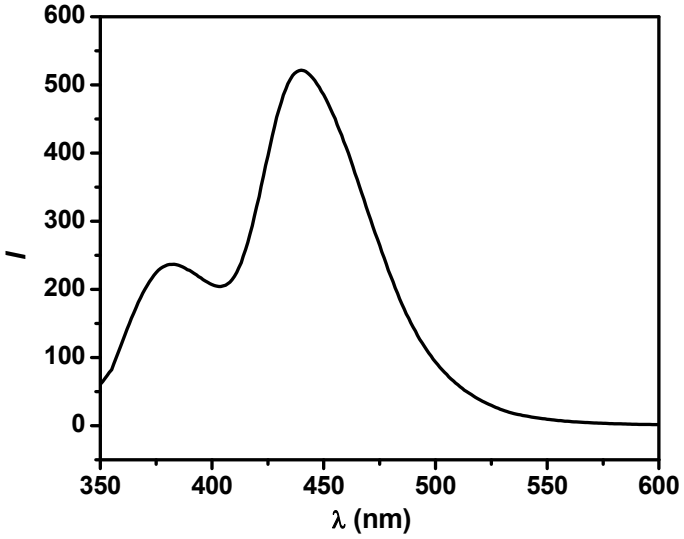

Figure S14. Fluorescence spectrum of L1 in MeCN (λ_{ex} = 330 nm).

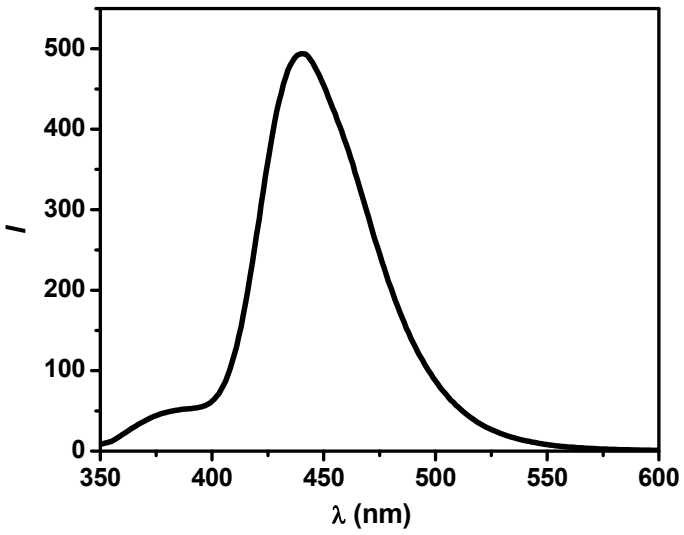

Figure S15. Fluorescence spectrum of L2 in MeCN (λ_{ex} = 330 nm).

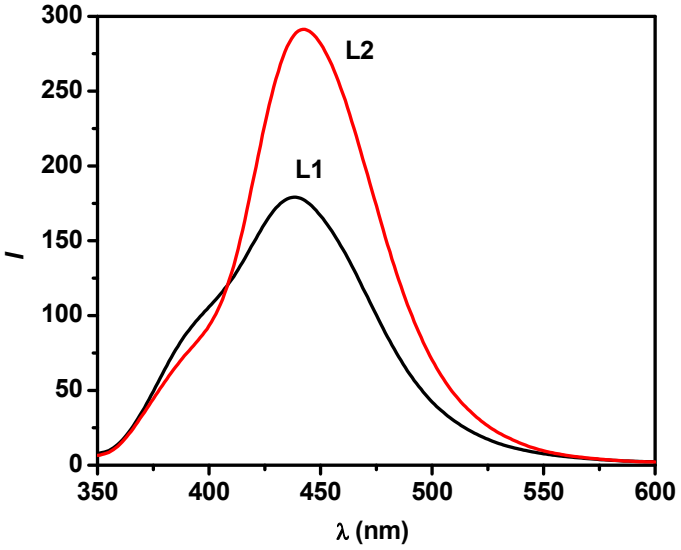

Figure S16. Fluorescence spectra of L1and L2 in PBS (λ_{ex} = 330 nm).

Fluorescence spectra of Cu^{2+} and Zn^{2+} complexes of L1 and L2

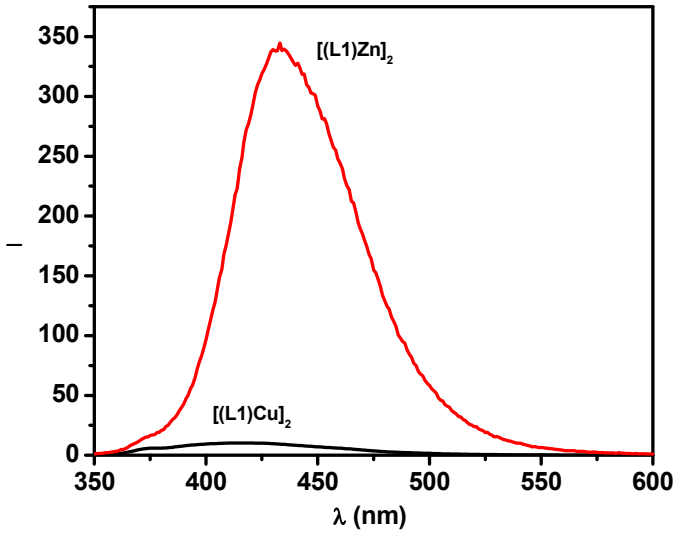

Figure S17. Fluorescence spectra of **1** and **2** in PBS (λ_{ex} 330 nm).

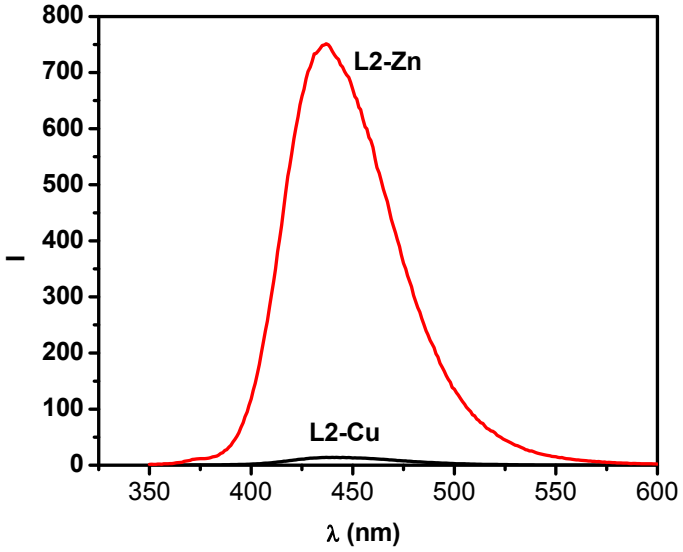

Figure S18. Fluorescence spectra of **3** and **4** in PBS (λ_{ex} 330 nm).

VII. ORTEP plots for 2 and 4

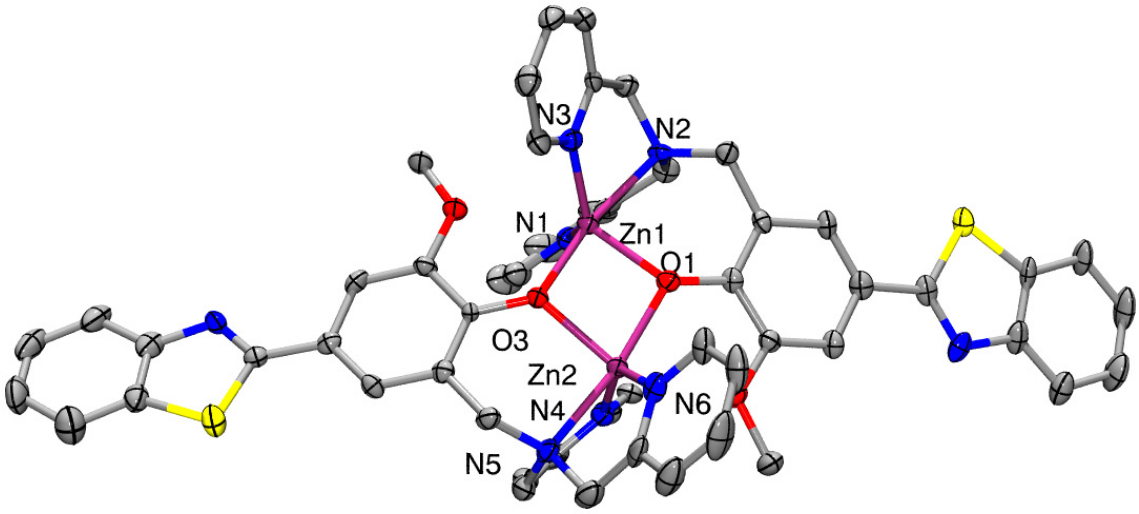

Figure S19. ORTEP plot of **2** with 30% thermal ellipsoids. Only one of the two unique molecules is shown; all hydrogen atoms, counteranions, and solvent molecules are omitted for clarity.

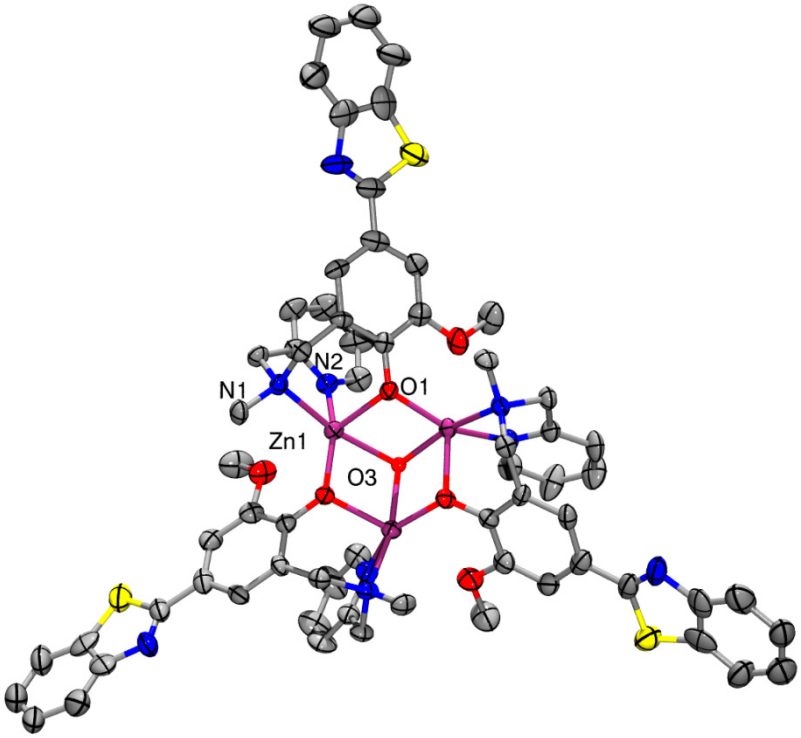

Figure S20. ORTEP view of **4** with 30% probability ellipsoids. All hydrogen atoms, counteranions, and solvent molecules are omitted for clarity.

VIII. Aβ fibril binding affinities of ThT, L1, and L2

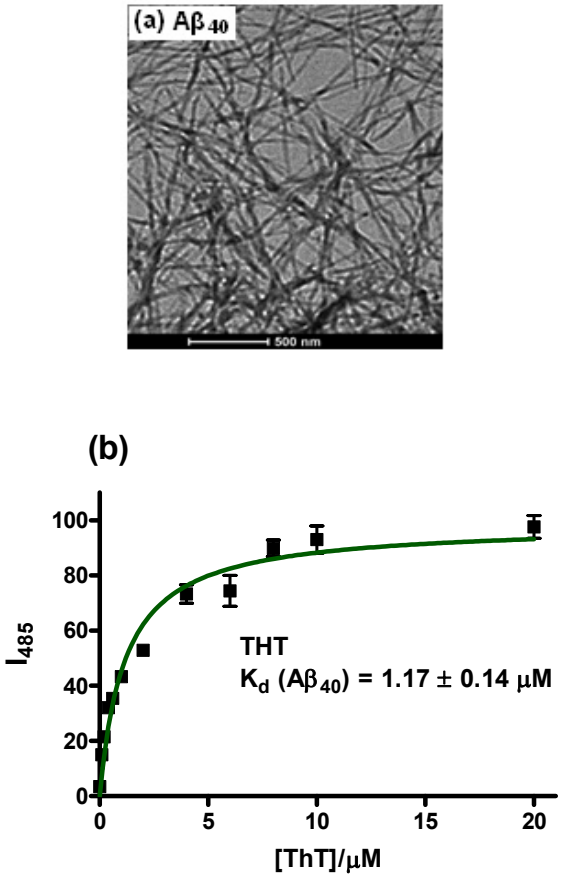

Figure S21. (a) TEM image of $A\beta_{40}$ fibrils; (b) Fluorescence assay of ThT binding to $A\beta_{40}$ fibrils (5 μM, PBS).

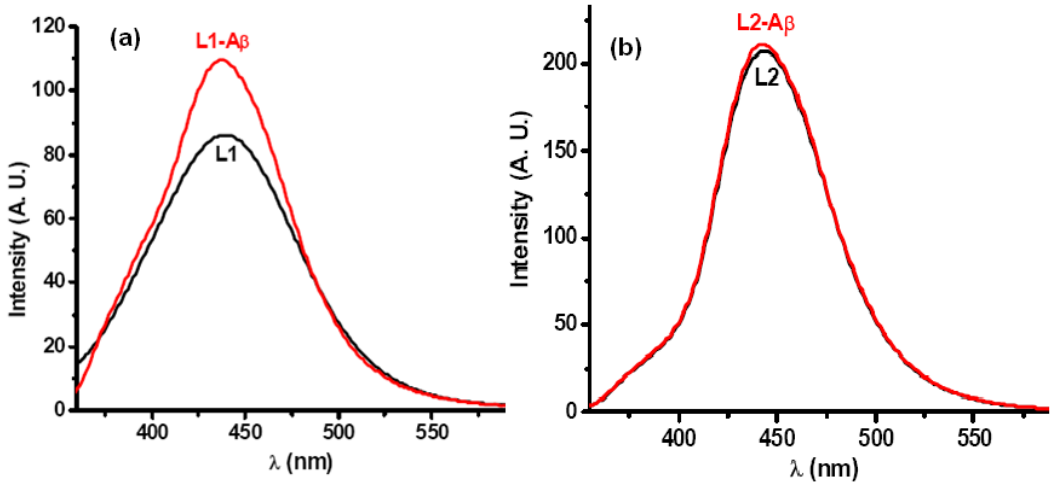

Figure S22. Change in fluorescence intensity of (a) L1 and (b) L2 with Aβ fibrils ([Aβ] = [L] = 2 μM, PBS).

Affinity of L1 and L2 for Zn-Aβ fibrils

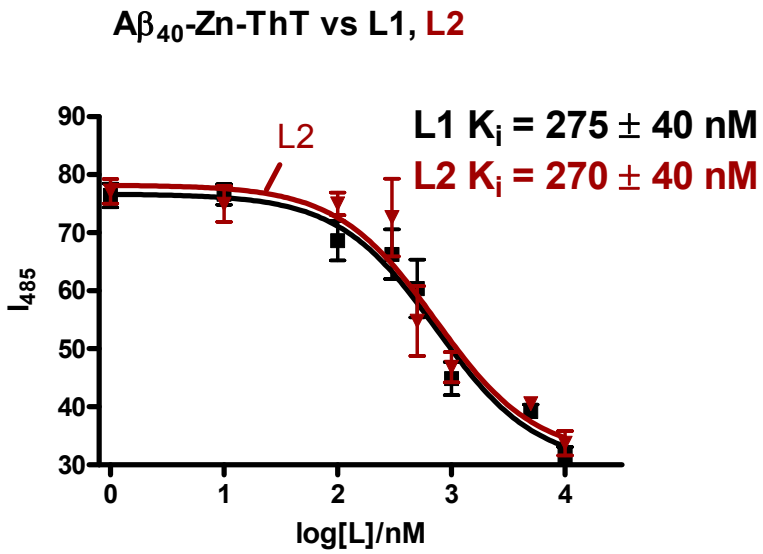

Figure S23. ThT fluorescence competition assays of L1 and L2 with $A\beta_{40}$ fibrils ([Aβ] = $[Zn^{+2}]$ = 5 μM, [ThT] = 2 μM, PBS).

IX. ThT Fluorescence of inhibition of Aβ aggregation by L1 and L2

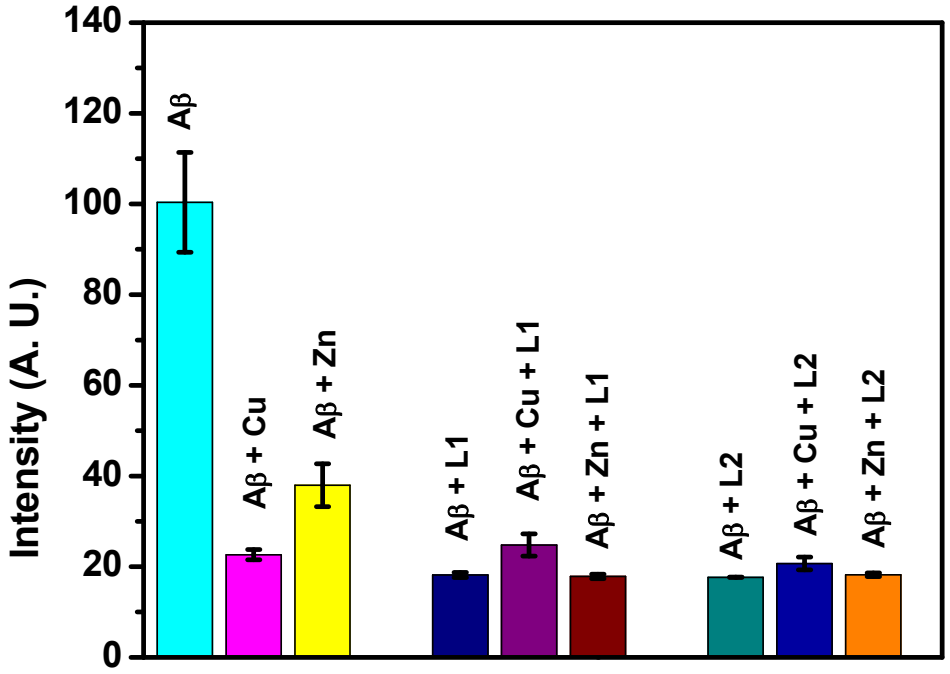

Figure 24. Normalized ThT fluorescence of inhibition of Aβ fibrillization, measured upon incubaton at 37 °C for 24h. Samples are as indicated on top of lanes (PBS, [Aβ] = 25 μM; [M^{2+}] = 25 μM; [compound] = 50 μM).

X. Peroxide production by Aβ, Cu, and compounds

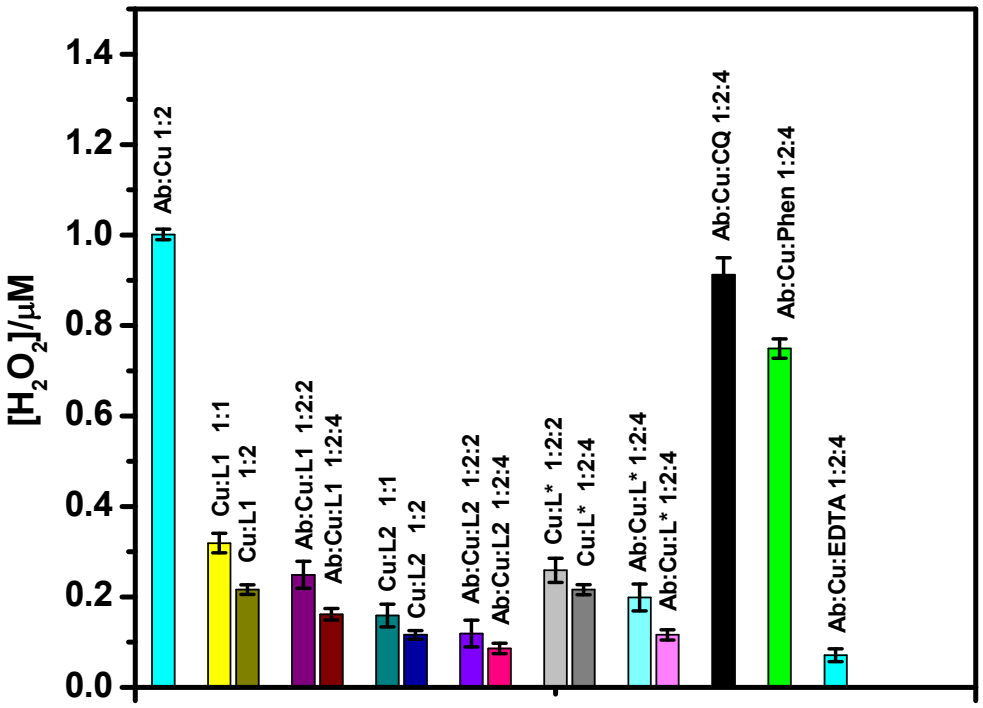

Figure S25. Normalized amounts of H_2O_2 produced in presence of Aβ, Cu, compounds, and sodium ascorbate, as determined by the Amplex-Red assay. [Aβ] = 200 nM, [Cu^{II}] = 400 nM, [chelator] = 400 or 800 nM, [ascorbate] = 10 μM, [Amplex-Red] = 50 nM, [HRP] = 0.1 U/mL. $\lambda_{ex}/_{em}$ = 530/590 nm. Abbreviations: L* = *N*-methyl-*N*,*N*-bis(2-pyridylmethyl)amine, CQ = clioquinol, phen = phenanthroline, EDTA = ethylenediaminetetraacetic acid.

XI. Cell viability assays for L1, L2, EDTA, and CQ

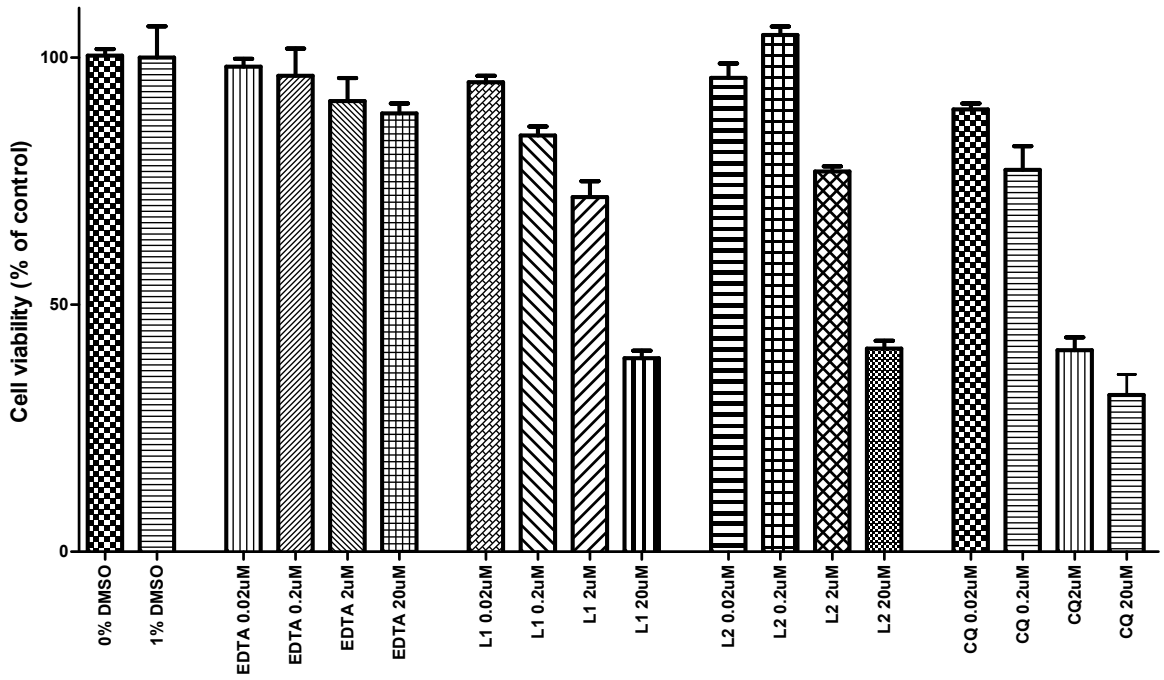

Figure S26. Cell viability (% control) upon incubation of Neuro2A cells with EDTA, L1, L2, and CQ without adding $A\beta_{42}$.

XII. TEM and Western analysis of inhibition of $A\beta_{42}$ aggregation by L1 and L2

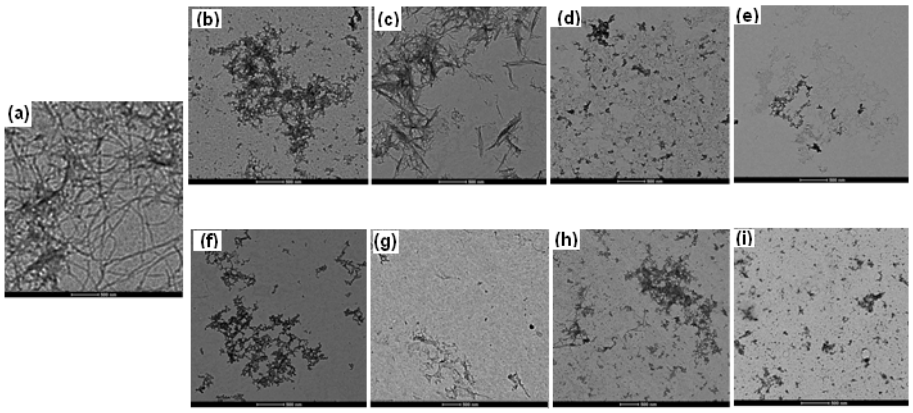

Figure S27. TEM images of the inhibition of $A\beta_{42}$ aggregation by substoichiometric L1 and L2, in the presence or absence of metal ions ($[A\beta_{42}] = [Cu^{2+}] = 25$ μM, [compound] = 2 or 10 μM, 37 °C, 24 h, scale bar = 500 nm). Samples: (a) $A\beta_{42}$; (b) $A\beta_{42}$ + L1 (2 μM); (c) $A\beta_{42}$ + L1 (10 μM); (d) $A\beta_{42}$ + L1 (2 μM) + Cu^{2+}; (e) $A\beta_{42}$ + L1 (10 μM) + Cu^{2+}; (f) $A\beta_{42}$ + L2 (2 μM); (g) $A\beta_{42}$ + L2 (10 μM); (h) $A\beta_{42}$ + L2 (2 μM) + Cu^{2+}; (i) $A\beta_{42}$ + L2 (10 μM) + Cu^{2+}.

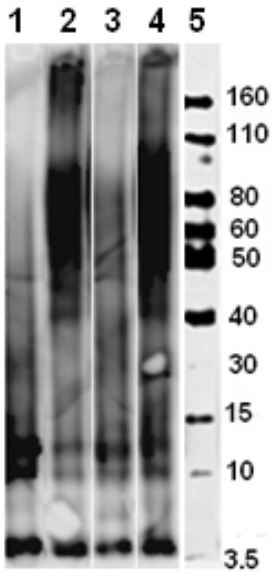

Figure S28. Native gel/Western blot analysis for the inhibition of $A\beta_{42}$ aggregation by substoichiometric L2, in the presence or absence of metal ions (($[A\beta_{42}] = [Cu^{2+}] = 25$ μM, [L2] = 2 or 10 μM, 37 °C, 24 h) (1) $A\beta_{42}$ + L2 (2 μM); (2) $A\beta_{42}$ + L2 (2 μM) + Cu^{2+}; (3) $A\beta_{42}$ + L2 (10 μM); (4) $A\beta_{42}$ + L2 (10 μM) + Cu^{2+}; (5) MW marker. Lanes 1-4 correspond to panels f-i in Fig S27, respectively.

XIII. X-ray structure data for $[(L1)Cu]_2(BPh_4)_2$ (1), $[(L1)Zn]_2(ClO_4)_2$ (2), $[(L2)_2Cu]$ (3), and $[(L2)_3Zn^{II}_3(O)]$ (ClO_4) (4)

Table S3. Bond lengths [Å] and angles [°] for $[(L1)Cu]_2(BPh_4)_2$ (1)

Cu(1)-N(1)	2.0024(19)
Cu(1)-N(2)	2.0179(18)
Cu(1)-N(3)	2.022(2)
Cu(1)-O(1)	2.1260(16)
Cu(1)-O(3)	1.9357(16)
Cu(2)-O(1)	1.9397(15)
Cu(2)-N(5)	1.985(2)
Cu(2)-N(6)	2.0281(19)
Cu(2)-N(7)	1.992(2)
Cu(2)-O(3)	2.1479(16)
O(3)-Cu(1)-N(1)	95.18(7)
O(3)-Cu(1)-N(2)	168.53(7)
N(1)-Cu(1)-N(2)	82.31(8)
O(3)-Cu(1)-N(3)	105.13(7)
N(1)-Cu(1)-N(3)	142.03(8)
N(2)-Cu(1)-N(3)	83.18(8)
O(3)-Cu(1)-O(1)	79.97(6)
N(1)-Cu(1)-O(1)	112.90(7)
N(2)-Cu(1)-O(1)	90.65(7)
N(3)-Cu(1)-O(1)	102.16(7)
O(1)-Cu(2)-N(5)	102.75(7)
O(1)-Cu(2)-N(7)	94.32(8)
N(5)-Cu(2)-N(7)	150.26(9)
O(1)-Cu(2)-N(6)	169.75(7)
N(5)-Cu(2)-N(6)	84.24(8)
N(7)-Cu(2)-N(6)	82.63(8)
O(1)-Cu(2)-O(3)	79.33(6)
N(5)-Cu(2)-O(3)	105.71(7)
N(7)-Cu(2)-O(3)	101.23(7)
N(6)-Cu(2)-O(3)	91.62(7)

Table S4. Bond lengths [Å] and angles [°] for $[(L1)Zn]_2(ClO_4)_2$ (2)

Zn(1)-N(3)	2.025(6)
Zn(1)-O(1)	2.032(5)
Zn(1)-O(3)	2.048(5)
Zn(1)-N(1)	2.066(6)
Zn(1)-N(2)	2.210(5)
Zn(1)-Zn(2)	3.085(1)
Zn(2)-O(1)	2.016(5)
Zn(2)-N(6)	2.037(6)
Zn(2)-O(3)	2.055(5)
Zn(2)-N(4)	2.069(6)
Zn(2)-N(5)	2.170(6)
Zn(2)-O(2)	2.446(5)
Zn(3)-O(7)	2.030(5)
Zn(3)-O(5)	2.031(5)
Zn(3)-N(9)	2.043(6)
Zn(3)-N(11)	2.056(7)
Zn(3)-N(10)	2.206(6)
Zn(3)-Zn(4)	3.070(1)
Zn(4)-O(5)	2.030(5)
Zn(4)-N(12)	2.034(6)
Zn(4)-O(7)	2.042(5)
Zn(4)-N(14)	2.046(6)
Zn(4)-N(13)	2.193(6)
N(3)-Zn(1)-O(1)	111.9(2)
N(3)-Zn(1)-O(3)	99.9(2)
O(1)-Zn(1)-O(3)	78.97(18)
N(3)-Zn(1)-N(1)	129.2(2)
O(1)-Zn(1)-N(1)	113.5(2)
O(3)-Zn(1)-N(1)	109.9(2)
N(3)-Zn(1)-N(2)	79.8(2)

O(1)-Zn(1)-N(2)	89.1(2)
O(3)-Zn(1)-N(2)	167.1(2)
N(1)-Zn(1)-N(2)	79.3(2)
N(3)-Zn(1)-Zn(2)	121.67(17)
O(1)-Zn(1)-Zn(2)	40.18(13)
O(3)-Zn(1)-Zn(2)	41.34(13)
N(1)-Zn(1)-Zn(2)	107.63(16)
N(2)-Zn(1)-Zn(2)	128.21(16)
O(1)-Zn(2)-N(6)	102.3(2)
O(1)-Zn(2)-O(3)	79.15(18)
N(6)-Zn(2)-O(3)	114.6(2)
O(1)-Zn(2)-N(4)	103.3(2)
N(6)-Zn(2)-N(4)	140.5(2)
O(3)-Zn(2)-N(4)	99.4(2)
O(1)-Zn(2)-N(5)	170.7(2)
N(6)-Zn(2)-N(5)	79.5(2)
O(3)-Zn(2)-N(5)	91.8(2)
N(4)-Zn(2)-N(5)	80.0(2)
O(1)-Zn(2)-O(2)	71.23(17)
N(6)-Zn(2)-O(2)	79.3(2)
O(3)-Zn(2)-O(2)	149.56(17)
N(4)-Zn(2)-O(2)	81.1(2)
N(5)-Zn(2)-O(2)	118.02(19)
O(1)-Zn(2)-Zn(1)	40.55(14)
N(6)-Zn(2)-Zn(1)	124.98(19)
O(3)-Zn(2)-Zn(1)	41.16(13)
N(4)-Zn(2)-Zn(1)	93.71(16)
N(5)-Zn(2)-Zn(1)	131.20(16)
O(2)-Zn(2)-Zn(1)	108.45(11)
O(7)-Zn(3)-O(5)	79.03(19)
O(7)-Zn(3)-N(9)	102.1(2)

O(5)-Zn(3)-N(9)	114.5(2)
O(7)-Zn(3)-N(11)	107.0(2)
O(5)-Zn(3)-N(11)	106.6(2)
N(9)-Zn(3)-N(11)	133.1(3)
O(7)-Zn(3)-N(10)	168.7(2)
O(5)-Zn(3)-N(10)	90.1(2)
N(9)-Zn(3)-N(10)	79.3(3)
N(11)-Zn(3)-N(10)	79.0(2)
O(7)-Zn(3)-Zn(4)	41.22(14)
O(5)-Zn(3)-Zn(4)	40.88(13)
N(9)-Zn(3)-Zn(4)	125.9(2)
N(11)-Zn(3)-Zn(4)	99.87(19)
N(10)-Zn(3)-Zn(4)	129.22(16)
O(5)-Zn(4)-N(12)	101.8(2)
O(5)-Zn(4)-O(7)	78.78(18)
N(12)-Zn(4)-O(7)	113.6(2)
O(5)-Zn(4)-N(14)	106.9(2)
N(12)-Zn(4)-N(14)	132.9(2)
O(7)-Zn(4)-N(14)	108.2(2)
O(5)-Zn(4)-N(13)	168.0(2)
N(12)-Zn(4)-N(13)	79.1(2)
O(7)-Zn(4)-N(13)	89.9(2)
N(14)-Zn(4)-N(13)	80.1(2)
O(5)-Zn(4)-Zn(3)	40.91(13)
N(12)-Zn(4)-Zn(3)	124.90(17)
O(7)-Zn(4)-Zn(3)	40.93(13)
N(14)-Zn(4)-Zn(3)	100.83(18)
N(13)-Zn(4)-Zn(3)	129.20(15)

Table S5. Bond lengths [Å] and angles [°] for $[(L2)_2Cu]$ (3)

Cu(1)-N(1)	2.563(5)
Cu(1)-O(1)	1.956(4)
Cu(1)-N(2)	2.102(4)
O(1)-Cu(1)-O(1)#1	180.0
O(1)-Cu(1)-N(2)	91.87(16)
O(1)#1-Cu(1)-N(2)	88.13(16)
O(1)-Cu(1)-N(2)#1	88.13(16)
O(1)#1-Cu(1)-N(2)#1	91.87(16)
N(2)-Cu(1)-N(2)#1	179.999(1)

Table S6. Bond lengths [Å] and angles [°] for $[(L2)_3Zn^{II}_3(O)](ClO_4)$ (4)

Zn(1)-O(1)#1	1.932(6)
Zn(1)-N(2)	2.026(7)
Zn(1)-O(1)	2.064(6)
Zn(1)-O(3)	2.142(4)
Zn(1)-N(1)	2.165(7)
O(1)#1-Zn(1)-N(2)	149.6(3)
O(1)#1-Zn(1)-O(1)	114.3(3)
N(2)-Zn(1)-O(1)	93.8(3)
O(1)#1-Zn(1)-O(3)	79.42(19)
N(2)-Zn(1)-O(3)	97.2(3)
O(1)-Zn(1)-O(3)	76.61(18)
O(1)#1-Zn(1)-N(1)	106.6(3)
N(2)-Zn(1)-N(1)	83.3(3)
O(1)-Zn(1)-N(1)	90.6(2)
O(3)-Zn(1)-N(1)	167.2(2)
C(1)-S(1)-C(7)	87.4(5)
C(11)-O(1)-Zn(1)#2	127.7(5)
C(11)-O(1)-Zn(1)	115.7(5)
Zn(1)#2-O(1)-Zn(1)	105.7(3)
C(12)-O(2)-C(15)	118.1(8)
Zn(1)#1-O(3)-Zn(1)	96.1(2)

XIV. Complete list of authors for references 8, 10, 44, 48, and 93.

(8) McGowan, E.; Pickford, F.; Kim, J.; Onstead, L.; Eriksen, J.; Yu, C.; Skipper, L.; Murphy, M. P.; Beard, J.; Das, P.; Jansen, K.; DeLucia, M.; Lin, W. L.; Dolios, G.; Wang, R.; Eckman, C. B.; Dickson, D. W.; Hutton, M.; Hardy, J.; Golde, T. *Neuron* **2005**, *47*, 191.

(10) Kuperstein, I.; Broersen, K.; Benilova, I.; Rozenski, J.; Jonckheere, W.; Debulpaep, M.; Vandersteen, A.; Segers-Nolten, I.; Van Der Werf, K.; Subramaniam, V.; Braeken, D.; Callewaert, G.; Bartic, C.; D'Hooge, R.; Martins, I. C.; Rousseau, F.; Schymkowitz, J.; De Strooper, B. *EMBO J.* **2010**, *29*, 3408.

(44) Cherny, R. A.; Atwood, C. S.; Xilinas, M. E.; Gray, D. N.; Jones, W. D.; McLean, C. A.; Barnham, K. J.; Volitakis, I.; Fraser, F. W.; Kim, Y. S.; Huang, X. D.; Goldstein, L. E.; Moir, R. D.; Lim, J. T.; Beyreuther, K.; Zheng, H.; Tanzi, R. E.; Masters, C. L.; Bush, A. I. *Neuron* **2001**, *30*, 665.

(48) Adlard, P. A.; Cherny, R. A.; Finkelstein, D. I.; Gautier, E.; Robb, E.; Cortes, M.; Volitakis, I.; Liu, X.; Smith, J. P.; Perez, K.; Laughton, K.; Li, Q.-X.; Charman, S. A.; Nicolazzo, J. A.; Wilkins, S.; Deleva, K.; Lynch, T.; Kok, G.; Ritchie, C. W.; Tanzi, R. E.; Cappai, R.; Masters, C. L.; Barnham, K. J.; Bush, A. I. *Neuron* **2008**, *59*, 43.

(92) Huang, X. D.; Cuajungco, M. P.; Atwood, C. S.; Hartshorn, M. A.; Tyndall, J. D. A.; Hanson, G. R.; Stokes, K. C.; Leopold, M.; Multhaup, G.; Goldstein, L. E.; Scarpa, R. C.; Saunders, A. J.; Lim, J.; Moir, R. D.; Glabe, C.; Bowden, E. F.; Masters, C. L.; Fairlie, D. P.; Tanzi, R. E.; Bush, A. I. *J. Biol. Chem.* **1999**, *274*, 37111.